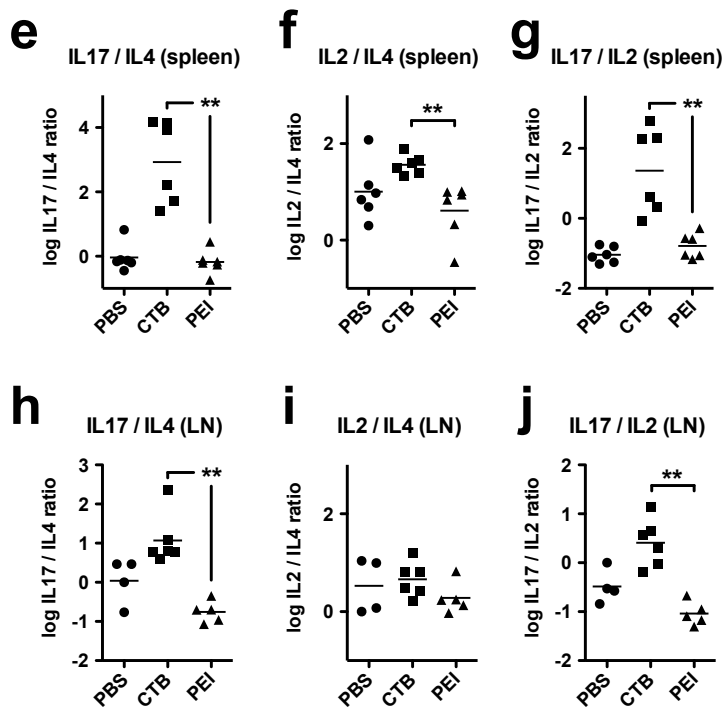
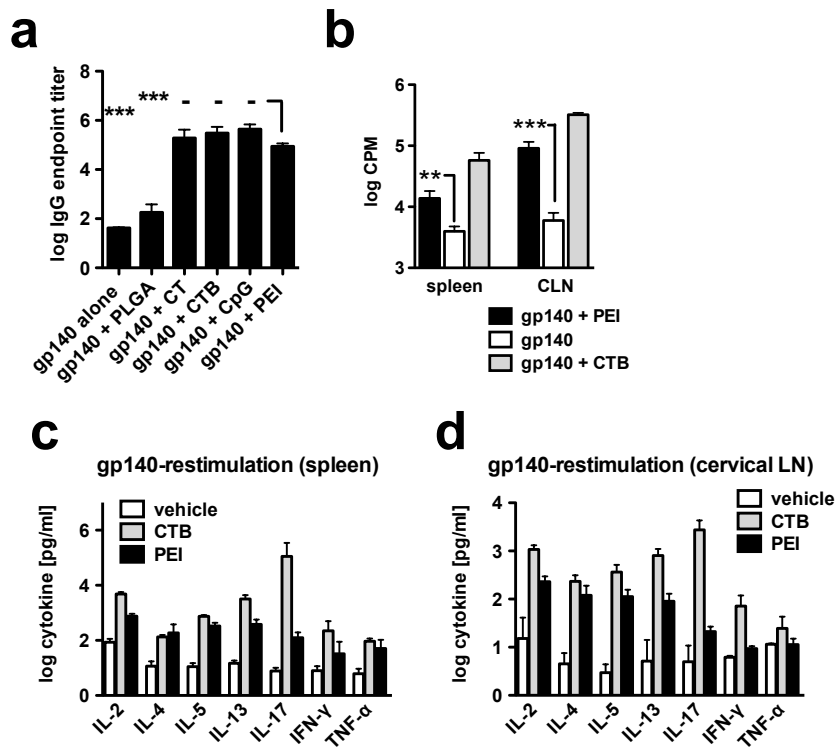
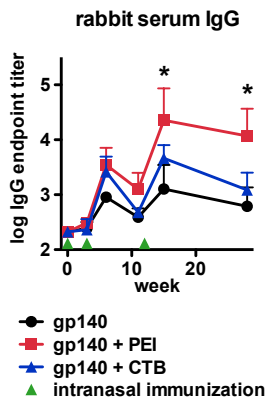
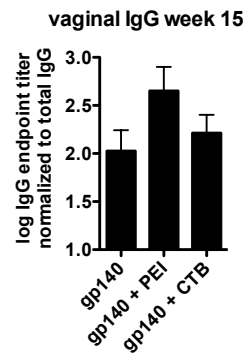


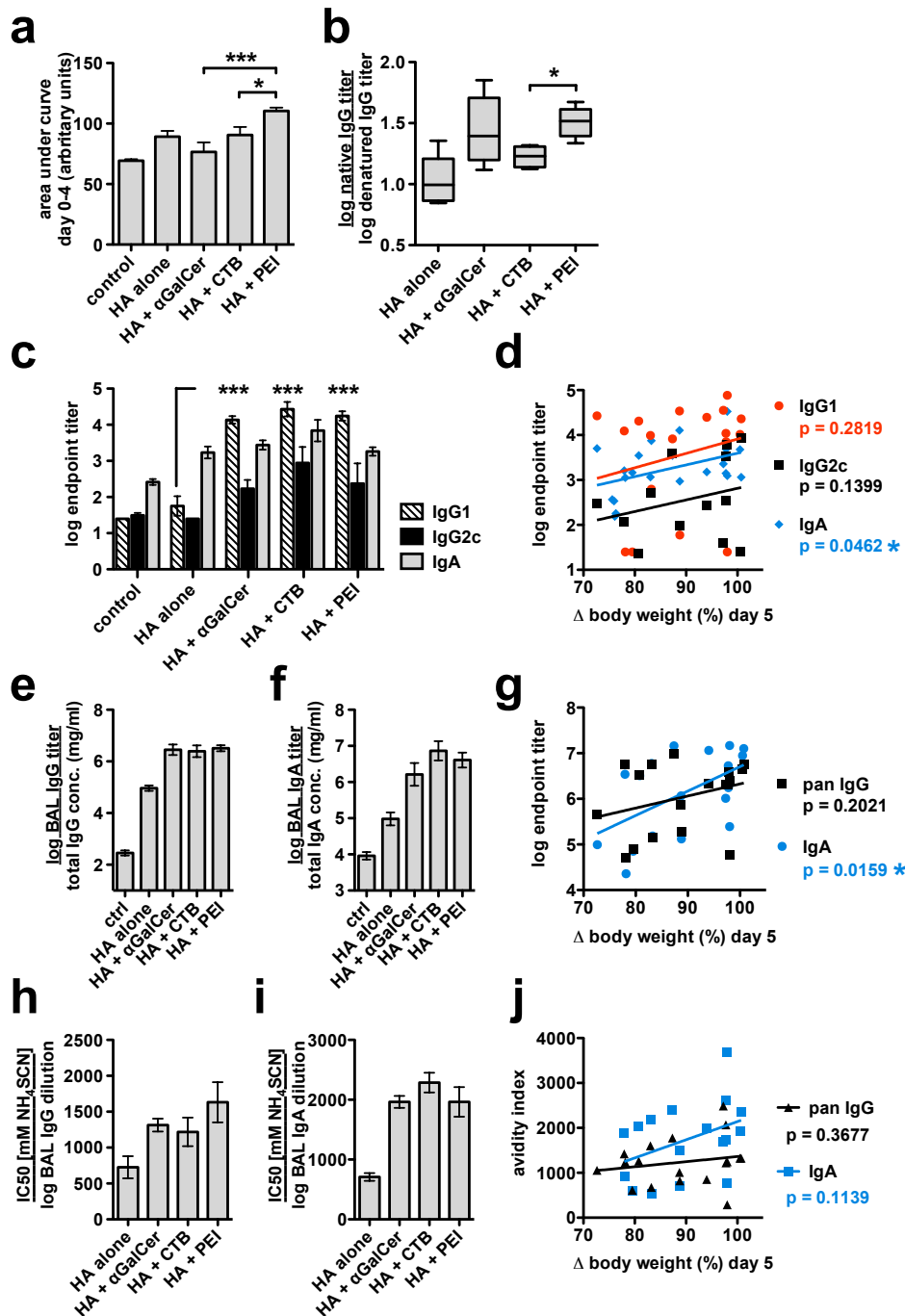
**Supplementary Figure 1.** Toxicity and immunogenicity of antigen-adjvant formulations. (a-c) Dose response of intranasal PEI toxicity and immunogenicity. BALB/c mice (n=4) were intranasally immunized with 10  $\mu$ g gp140 alone or co-formulated with the indicated quantity of PEI. (a) Weight loss as measure of toxicity. (b) Area under the weight loss curves depicted in (a) of individual mice as a measure of toxicity over time. (c) gp140-specific serum IgG responses as a measure of immunogenicity. (d-e) BALB/c mice (n=5) were immunized intranasally with 10  $\mu$ g HIV-1 gp140 combined with 20  $\mu$ g CTB, CpG, PEI, 2  $\mu$ g CT or 1 mg PLGA nanoparticles (same mice as in Fig. 1c-f). (d) Weight loss after priming immunization as measure of toxicity. (e) Area under the weight loss curves depicted in (d) of individual mice as a measure of toxicity over time. (f) H&E stained cross-sections of the mouse NALT region. BALB/c mice (n=2) were immunized intranasally with 10  $\mu$ g ovalbumin alone (PBS) or in combination with 20  $\mu$ g PEI (large image and PEI) or 10  $\mu$ g CpG-ODN (CpG) and sacrificed for histology 24 h post immunization. The epithelial region depicted in the small insets is indicated by a black square in the main image. Bar: black 200  $\mu$ m, white 25  $\mu$ m. AU, arbitrary units; Data are presented as mean values of replicates  $\pm$  SEM; ns, - = not significant; \* p<0.05.



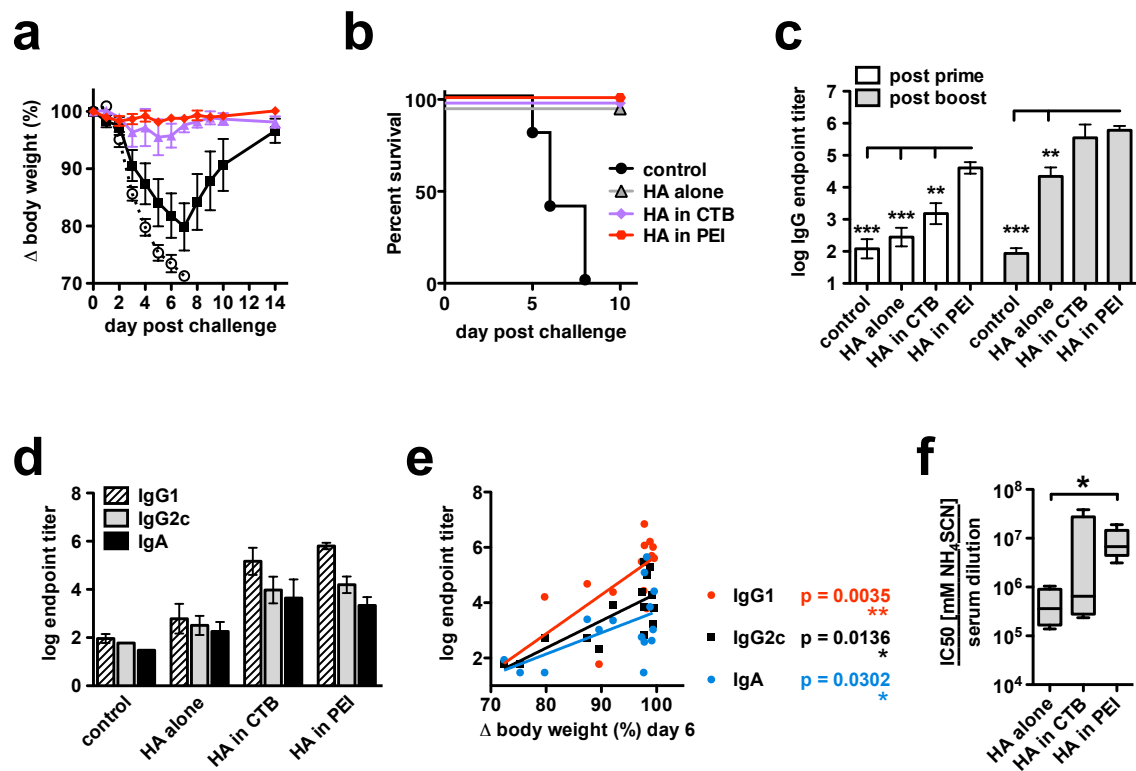
**Supplementary Figure 2.** Antigen-specific responses of gp140-immunized mice. (a) BALB/c mice (n=5) were immunized intranasally with two doses of 10  $\mu$ g HIV-1 gp140 combined with, 20  $\mu$ g CTB, CpG, PEI, 2  $\mu$ g CT or 1 mg PLGA nanoparticles and endpoint titers were determined 2 weeks post the final immunization (same mice as in Fig. 1c-f). (b-j) BALB/c mice (n=6) were immunized intranasally with three doses of gp140 alone or adjuvanted with CTB or PEI (same mice as in Fig. 1g). (b) Proliferation of gp140-restimulated splenocytes or cervical lymph node (CLN) cells from immunized mice shown by  $^3$ H-thymidine incorporation (Anova/Dunnett). (c-d) Cytokine production of gp140-restimulated splenocytes (c) or CLN cells (d) assayed by multiplex Th1/Th2 cytokine bead array. Splenocyte culture (e-g) or CLN culture (h-j) cytokine ratios of individual mice (Kruskal-Wallis/Dunn test), (e,h) IL17 / IL4 ratio, (f,i) IL2 / IL4 ratio, (g,j) IL17 / IL2 ratio. Data are presented as mean  $\pm$  SEM; - = not significant; \*\* p<0.01, \*\*\* p<0.001.

**a****b****Supplementary Figure 3.**

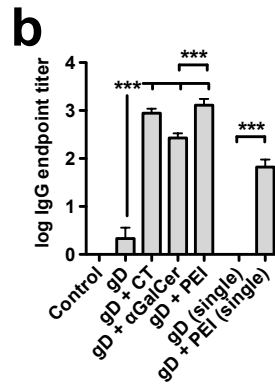
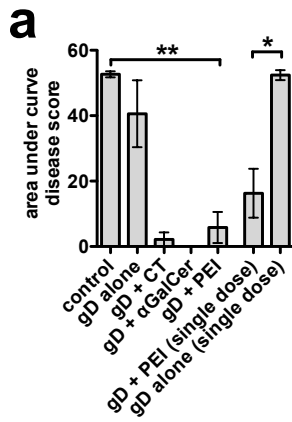
Mucosal adjuvant activity of PEI in rabbits. New Zealand White Rabbits (n=4) were immunized intranasally at weeks 0 and 3 with 50  $\mu$ g, and at week 12 with 25  $\mu$ g gp140 alone or in combination with 100  $\mu$ g PEI or CTB. (a) gp140-specific serum IgG endpoint titer time course (two way ANOVA/Bonferroni). (b) gp140-specific vaginal IgG endpoint titers at week 15. Data are presented as mean  $\pm$  SEM; \*p<0.05.



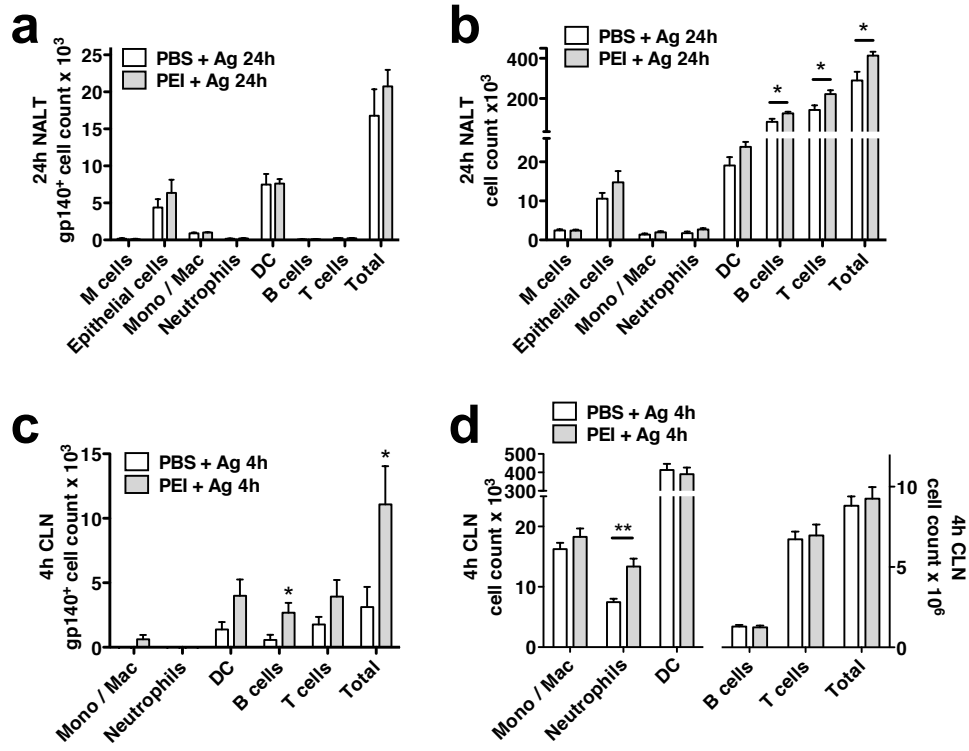
**Supplementary Figure 4.** Weight loss and serological responses of mice receiving a single immunization with HA alone or combined with adjuvant followed by influenza virus challenge (same mice as **Fig. 1h,i**). **(a)** Day 0-4 weight loss quantified by area under curve for individual mice (Kruskal-Wallis/Dunn test). **(b)** Ratio of serum IgG endpoint titers against native versus SDS/DTT-denatured HA (Anova/Bonferroni). **(c)** HA-specific serum IgG1, IgG2c or IgA prior to influenza challenge. **(d)** Correlation between log-transformed anti-HA serum immunoglobulin titer and the percentage of the original body weight on day 5 post-virus challenge (Spearman-correlation of log-transformed titers). **(e)** HA-specific BAL IgG or **(f)** IgA at euthanization. **(g)** Correlation between log-transformed anti-HA BAL immunoglobulin titer and the percentage of the original body weight on day 5 post-virus challenge (Spearman-correlation of log-transformed titers). **(h,i)** Avidity index was determined by titrating a chaotropic agent (NH<sub>4</sub>SCN) onto bronchoalveolar lavage (BAL) IgG **(h)** or IgA **(i)** pre-bound to immobilized HA; data were normalized to the log specific endpoint dilution of each BAL sample determined in e-f. **(j)** Correlation between BAL normalized avidity index and the percentage of the original body weight on day 5 post-virus challenge (Spearman-correlation of log-transformed titers). Data are presented as mean ± SEM; ns = not significant; \*p<0.05, \*\*p<0.01, \*\*\* p<0.001.



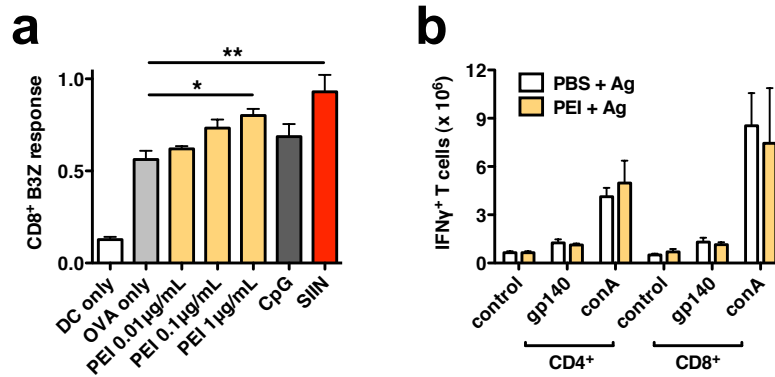
**Supplementary Figure 5.** Protection of mice from highly pathogenic influenza challenge. C57Bl/6 mice (n=5) were immunized intranasally with two doses of 10  $\mu$ g influenza A (PR8) HA alone or combined with 10  $\mu$ g CpG, 20  $\mu$ g CTB or 20  $\mu$ g PEI, followed by intranasal challenge four weeks later with a highly pathogenic dose of live influenza A PR8 virus. (a) Weight loss post-challenge. (b) Kaplan-Meier survival plots. (c) HA-specific serum IgG before challenge (Anova/Dunnett test). (d) HA-specific serum IgG1, IgG2c or IgA titers before challenge. (e) Correlation between anti-HA immunoglobulin titer and the percentage of the original body weight on day 6 post-virus challenge (Spearman-correlation of log-transformed titers). (f) Avidity index was determined by titrating a chaotropic agent (NH<sub>4</sub>SCN) onto immune serum IgG pre-bound to immobilized HA; high avidity interactions can tolerate higher chaotropic agent concentrations than low avidity interactions. Avidity index was normalized to the dilution of each immune serum used. Data are presented as mean  $\pm$  SEM; \*p<0.05, \*\* p<0.01, \*\*\* p<0.001.



**Supplementary Figure 6.** Disease score after HSV-2 challenge and serological responses to HSV-2 gD immunization (same mice as in **Fig. 1j,k**). **(a)** Disease score (from **Fig. 1j**) was quantified as area under the curve for individual mice **(b)** gD-specific serum IgG titers from mice 3 weeks post-final immunization (Anova/Bonferroni). Data are presented as mean  $\pm$  SEM; \* $p$ <0.05; \*\* $p$ <0.01, \*\*\* $p$ <0.001.

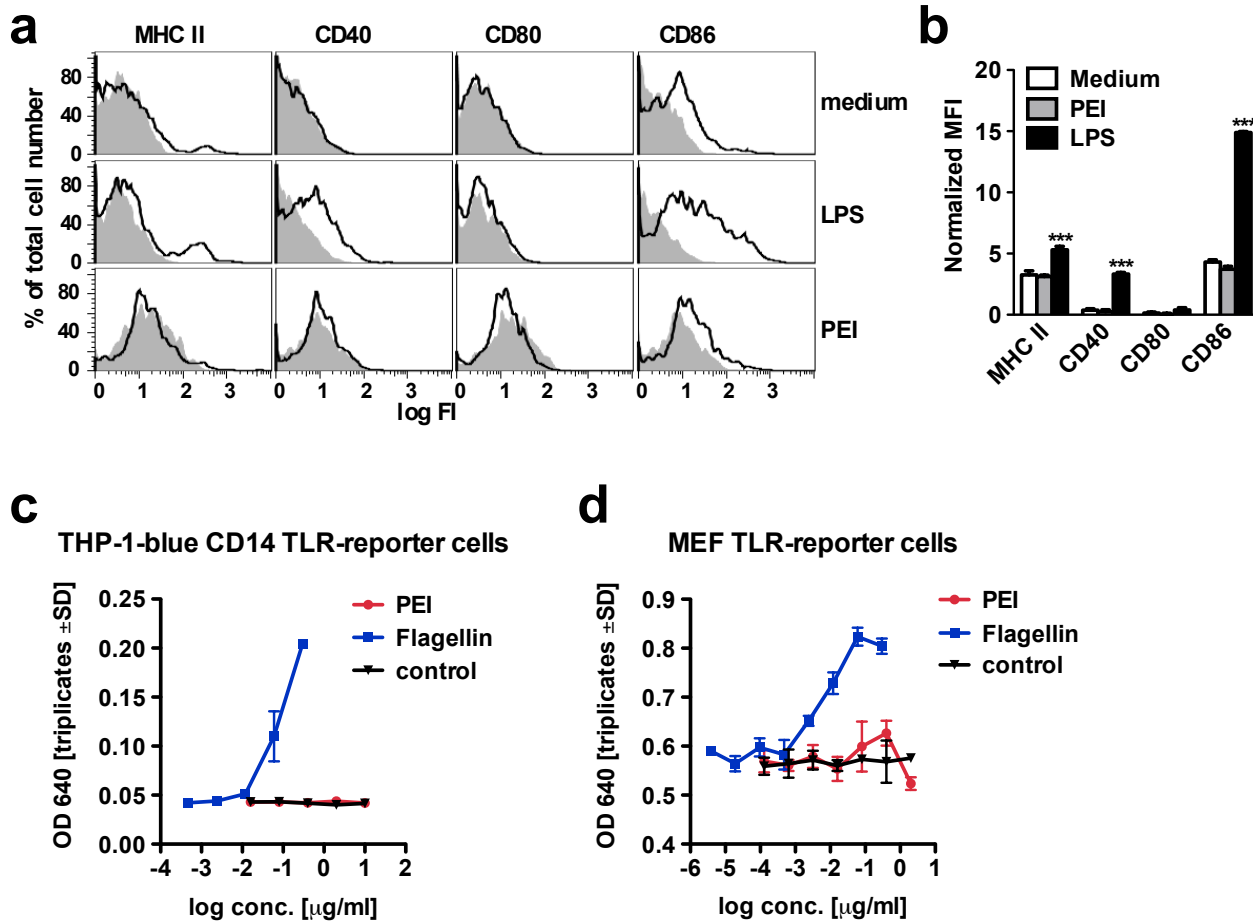


**Supplementary Figure 7.** Uptake of gp140<sub>647</sub> into NALT (a) or CLN (c) cells, or cell recruitment into NALT (b) or CLN (d), 24 h (a-b) or 4 h (c-d) after intranasal immunization of BALB/c mice with 10 µg gp140<sub>647</sub> ± 20 µg PEI (same mice as in Fig. 2h-k, n=5, two-tailed *t*-test). Leukocyte populations were identified by flow cytometry with appropriate labeling and gates. Data are representative of 2 or more independent experiments and are presented as mean values of replicates from one experiment ± SEM; \* *p*<0.05, \*\* *p*<0.01.

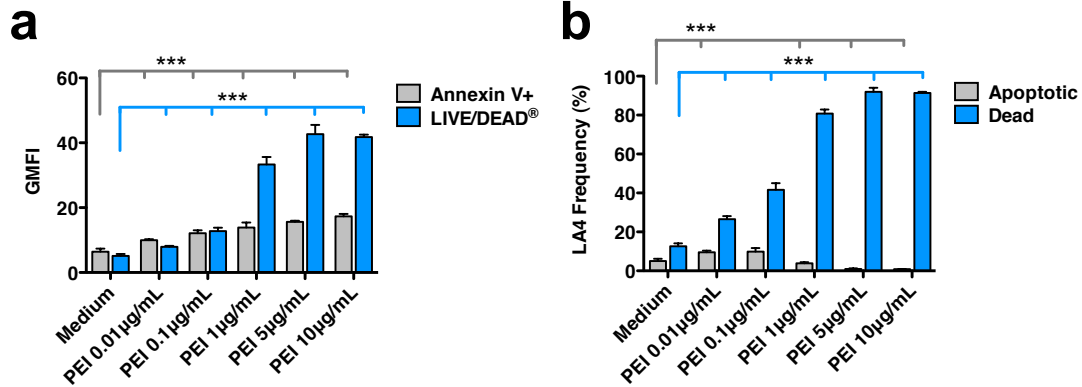


**Supplementary Figure 8.** Antigen cross-presentation and *in vivo* T cell induction. **(a)** Splenic DC were pulsed with OVA alone, OVA pre-complexed with PEI (0.002 – 0.2  $\mu\text{g}/\text{mL}$ ), in the presence of CpG or SIINFEKL peptide (SIIN) and co-incubated with the *lacZ*-inducible SIINFEKL-specific CD8<sup>+</sup> T cell hybridoma B3Z. Hybridoma responses were assessed via intracellular  $\beta$ -galactosidase activity. **(b)** C57Bl/6 mice were immunized four times intranasally with 10  $\mu\text{g}$  gp140 alone or complexed with 20  $\mu\text{g}$  PEI. 2 weeks post-final immunization, CLN cells were restimulated with gp140 or concanavalin A for 4 h before Brefeldin A was added and cells were incubated for a further 18 h. Intracellular IFN- $\gamma$  expression was determined by flow cytometry and leukocyte populations were identified by appropriate labeling and gates. Data are presented as mean  $\pm$  SEM; \*  $p < 0.05$ , \*\*  $p < 0.01$ .

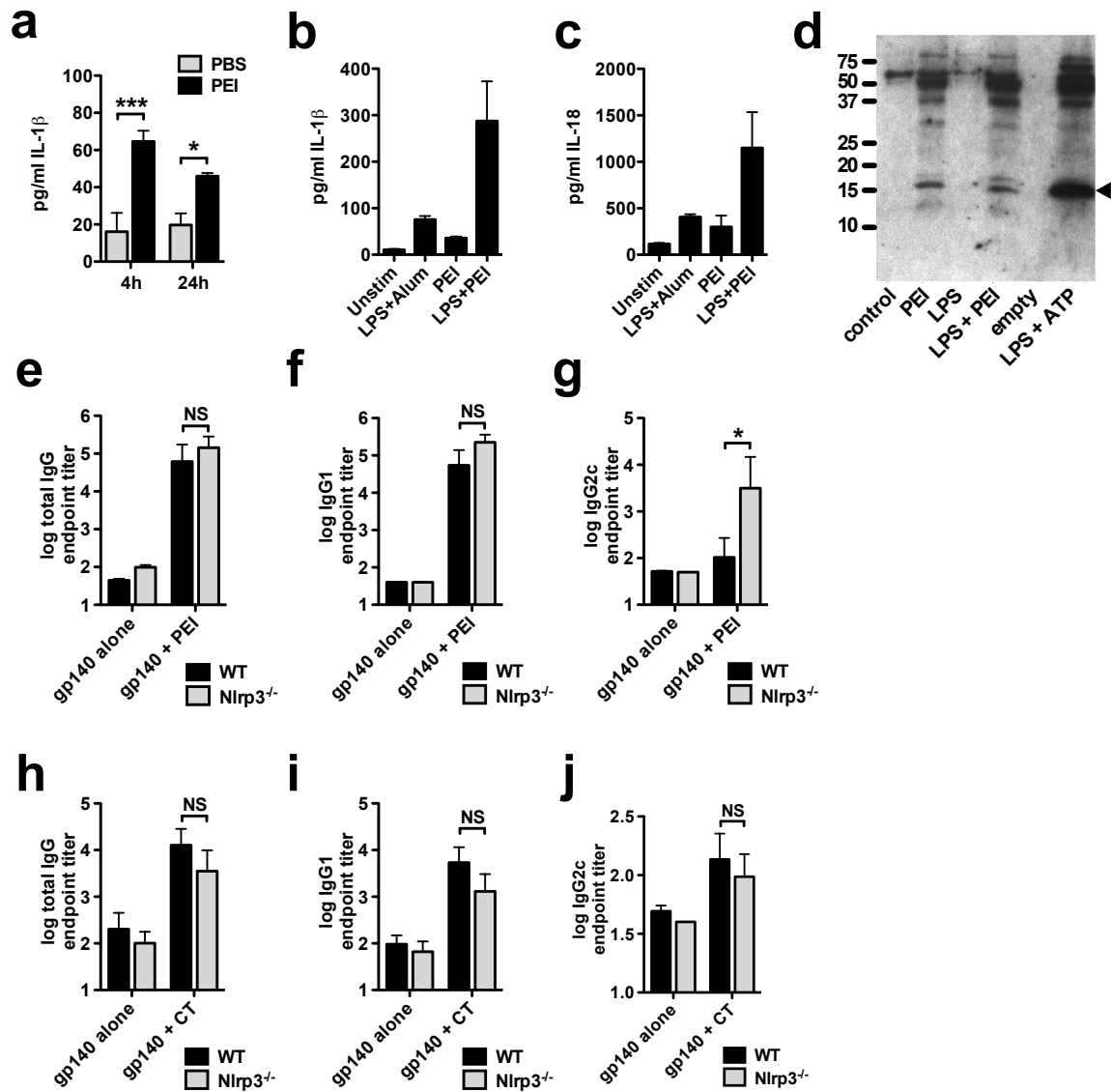




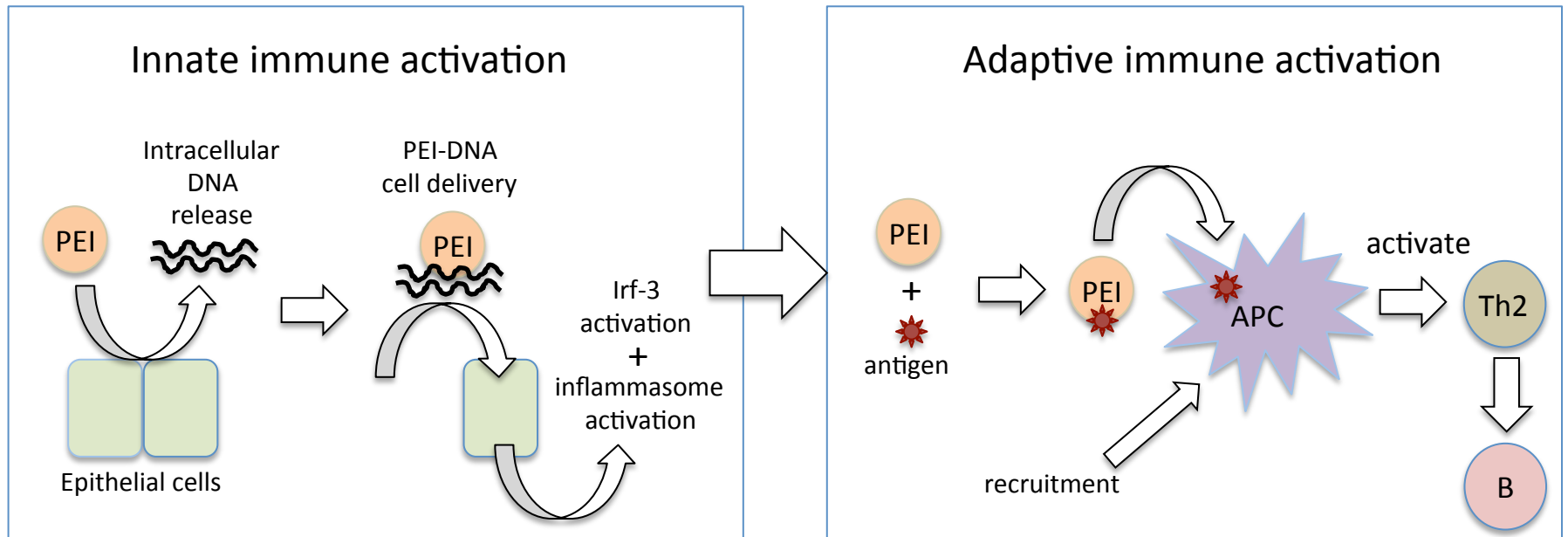
**Supplementary Figure 9.** PEI neither induces DC maturation nor directly activates TLRs. (a) BMDC isolated from BALB/c mice were incubated for 16 h with 2  $\mu\text{g/ml}$  PEI or 1  $\mu\text{g/ml}$  LPS, washed and analyzed by flow cytometry. Data are representative of three independent experiments. (b) Mean fluorescence intensity (MFI) of stained BMDC normalized to relevant isotype controls (Anova/Bonferroni). (c) THP-1 blue CD14 TLR reporter cells or (d) mouse embryonic fibroblast (MEF) TLR reporter cells were incubated overnight with PEI, flagellin or medium alone and reporter gene activation was determined (representative of two independent experiments performed in triplicate). Responsiveness of THP-1 and MEF cells was tested using a panel of specific TLR agonists and results were consistent with the supplier's specifications (data not shown). Data are presented as mean  $\pm$  SD; \*\*\*  $p < 0.001$ .



**Supplementary Figure 10.** Epithelial cytotoxicity is induced by overnight exposure to PEI *in vitro*. Cell death and apoptosis were detected by LIVE/DEAD® staining and Annexin V binding respectively. **(a)** The geometric mean fluorescence intensity (GMFI) of single positive Annexin V<sup>+</sup> cells and cells positive for the cell death marker (LIVE/DEAD®) 18 h after PEI exposure. **(b)** The frequency of apoptotic (Annexin V<sup>+</sup>LIVE/DEAD®<sup>-</sup>) cells and dead cells (LIVE/DEAD<sup>+</sup>) 18 h after PEI exposure. Data are presented as mean ± SD; \*\*\* p<0.001.



**Supplementary Figure 11.** PEI activates the NLRP3 inflammasome. **(a)** Peritoneal lavage cytokine induction 4 h or 24 h after peritoneal PEI injection (80  $\mu$ g, n=5, Anova/Bonferroni). **(b, c)** PEI-induced cytokine production by bone marrow-derived macrophages (BMM). BMM in quadruplicate cultures were LPS-stimulated overnight followed by incubation with 15  $\mu$ g/mL Alhydrogel (Alum), 20  $\mu$ g/mL PEI for 4 h or 10  $\mu$ g/mL ATP for 30 min. IL-1 $\beta$  **(b)** and IL-18 **(c)** were measured in supernatants by ELISA. **(d)** Cleaved Caspase-1 p10 (17 kDa, marked with arrow) in cell lysates was visualized by immunoblot; data are representative of three independent experiments. **(e-g)** gp140-specific serum immunoglobulin responses of C57BL/6 wt or Nlrp3<sup>-/-</sup> mice (n=5, Anova/Dunnett). Mice received two intranasal immunizations with 10  $\mu$ g (first) and 5  $\mu$ g gp140 (second immunization) alone or complexed with 20  $\mu$ g PEI. gp140-specific serum pan IgG **(e)**, IgG1 **(f)**, IgG2c **(g)** titers (Anova/Bonferroni) 2 weeks post final immunization. **(h-j)** gp140-specific serum immunoglobulin responses of C57BL/6 wt (n=3) or Nlrp3<sup>-/-</sup> mice (n=6, Anova/Dunnett). Mice received two intranasal immunizations with 10  $\mu$ g (first) and 5  $\mu$ g gp140 (second immunization) alone or with 2  $\mu$ g CT. gp140-specific serum pan IgG **(h)**, IgG1 **(i)**, IgG2c **(j)** titers (Anova/Bonferroni) 2 weeks post final immunization. Data are presented as mean  $\pm$  SEM; NS, not significant; \*p<0.05; \*\*\* p<0.001.



**Supplementary Figure 12.** Proposed model for PEI activation of innate and adaptive immune responses. Left panel, PEI triggers release of cellular DNA that complexes with PEI and is taken up into other cells. PEI delivers the DNA to the cytosol where it activates DNA sensors that drive an Irf-3-dependent immune activation program. The NLRP3 inflammasome is also activated. In parallel, PEI associates with glycoprotein antigen and complexes are targeted to, and taken up by APC. These then process the antigen via the HLA class-II pathway leading to activation of Th2 cells. Th2 cells provide help for B cells to produce antibodies against the antigen.